International Journal of Heat and Mass Transfer 52 (2009) 1887–1896

Contents lists available at ScienceDirect

International Journal of Heat and Mass Transfer

journal homepage: www.elsevier.com/locate/ijhmt

Non-Darcian effects on natural convection heat transfer in a wavy porous enclosure

Khalil Khanafer [a], Bader Al-Azmi [b], Alia Marafie [b], Ioan Pop [c,*]

[a] Vascular Mechanics Laboratory, Department of Biomedical Engineering, University of Michigan, Ann Arbor, MI 48109, USA
[b] Mechanical Engineering Department, Kuwait University, Al-Safat 13060, Kuwait
[c] Faculty of Mathematics, University of Cluj, R-3400 Cluj, Romania

ARTICLE INFO

Article history:
Received 20 February 2008
Received in revised form 12 July 2008
Available online 16 December 2008

ABSTRACT

A numerical investigation is carried out to analyze natural convection heat transfer inside a cavity with a sinusoidal vertical wavy wall and filled with a porous medium. The vertical walls are isothermal while the top and bottom horizontal straight walls are kept adiabatic. The transport equations are solved using the finite element formulation based on the Galerkin method of weighted residuals. The validity of the numerical code used is ascertained by comparing our results with previously published results. The importance of non-Darcian effects on convection in a wavy porous cavity is analyzed in this work. Different flow models for porous media such, as Brinkman-extended Darcy, Forchheimer-extended Darcy, and the generalized flow models, are considered. Results are presented in terms of streamlines, isotherms, and local heat transfer. The implications of Rayleigh number, number of wavy surface undulation and amplitude of the wavy surface on the flow structure and heat transfer characteristics are investigated in detail while the Prandtl number is considered equal to unity.

1. Introduction

Flow and heat transfer from irregular surfaces are often encountered in many engineering applications to enhance heat transfer such as micro-electronic devices, flat-plate solar collectors and flat-plate condensers in refrigerators [1], and geophysical applications (e.g., flows in the earth's crust [2]), underground cable systems, electric machinery, cooling system of micro-electronic devices, etc. In addition, roughened surfaces could be used in the cooling of electrical and nuclear components where the wall heat flux is known. It is worth noting that most of the previous studies on natural convection inside a wavy enclosure were conducted in the absence of porous medium [2–5]. Adjlout et al. [3] have studied laminar natural convection in an inclined cavity with a heated undulated wall, i.e., smooth wave-like pattern. Their results concluded that the wavy wall affects the flow and heat transfer rate in the enclosure. Mahmud et al. [4] studied flow and heat transfer characteristics inside an isothermal vertical wavy-walled enclosure bounded by two adiabatic straight walls at different Grashof number and orientations for some selected waviness of the surface. Das and Mahmud [2] conducted a numerical investigation of natural convection in an enclosure consisting of two isothermal horizontal wavy walls and two adiabatic vertical straight walls. They reported that the amplitude-wavelength ratio affected local heat transfer rate, but it had no significant influence on average heat transfer rate. Dalal and Das [5] analyzed numerically natural convection in a cavity with a wavy vertical wavy wall heated from below and uniformly cooled from top and both vertical sides. Their results showed that the presence of undulation in the right wall affected local heat transfer rate and flow field as well as thermal field.

Natural convective flow in differentially heated enclosures filled with Darcian or non-Darcian fluid-saturated porous media has received a considerable attention in the literature. This attention stems from its importance in vast technological, engineering, and natural applications. The steady-state free convection inside a cavity made of two horizontal straight walls and two vertical bent-wavy walls and filled with a fluid-saturated porous medium was numerically investigated by Misirlioglu et al. [6] using Darcy model. Later on, the same authors analyzed numerically natural convection inside an inclined wavy enclosure filled with a porous medium assuming Darcy flow model with the Boussinesq approximation [7]. Their results showed that the flow and thermal structures was found to be highly dependent on surface waviness for inclination angles less than 45°, especially for high Rayleigh numbers. Kumar et al. [8] studies numerically free convection heat transfer from am isothermal wavy surface in a porous enclosure assuming valid Forchheimer-extended Darcy model. The average Nusselt number was found to increase with increasing Rayleigh number whereas it decreased with increasing value of wave amplitude. The effect of surface undulations on natural convection in a thermally stratified vertical porous enclosure has been analyzed numerically by Kumar and Shalini [9] using finite element method. The flow was modeled using Darcy model. The results of that study illustrated that the global heat transfer into the system has been

* Corresponding author. Tel.: +40 264 594 315; fax: +40 264 591 906.
E-mail address: pop.ioan@yahoo.co.uk (I. Pop).

0017-9310/$ - see front matter © 2008 Elsevier Ltd. All rights reserved.
doi:10.1016/j.ijheatmasstransfer.2008.08.040

Nomenclature

A	amplitude of the wavy surface
c_p	specific heat at constant pressure
Da	Darcy number, K/H^2
F	Forchheimer constant
G	acceleration due to gravity
H	height of the cavity
J	unit vector oriented along the pore velocity vector
K	thermal conductivity
K	permeability of the porous medium
L	length of the cavity
N	number of undulation
Nu	Nusselt number
p	pressure
P	dimensionless pressure, $p/\rho(g\beta\Delta TH)$
Pr	Prandtl number, ν/α
Ra	Rayleigh number, $g\beta\Delta TH^3/\nu\alpha$
t	time
T	temperature
T_C	temperature of the cold wall
T_H	temperature of the hot wall
$\mathbf{v}$	dimensional velocity vector
$\mathbf{V}$	dimensionless velocity vector, $\mathbf{v}/\sqrt{g\beta\Delta TH}$
W	dimensionless width of the wall, b/H
x	x-coordinate
X	dimensionless X-coordinate, x/H
y	y-coordinate
Y	dimensionless Y-coordinate, y/H

Greek symbols

α	thermal diffusivity
β	coefficient of thermal expansion
ε	porosity of the porous medium
ν	kinematic viscosity
θ	dimensionless temperature, $(T - T_C)/(T_H - T_C)$
ρ	density
τ	dimensionless time, $t\sqrt{g\beta\Delta TH/H}$

found to decrease with increasing amplitude and increasing number of waves per unit length. Kumar [10] analyzed numerically using finite element method free convection induced by a vertical wavy surface with uniform heat flux in a porous enclosure. The results revealed that small sinusoidal drifts from the smoothness of a vertical wall with a phase angle of 60° and high frequency enhanced the free convection from a vertical wall with uniform heat flux.

Murthy et al. [11] studied the effect of surface undulations on the natural convection heat transfer from an isothermal surface in a Darcian fluid-saturated porous enclosure assuming valid Darcy flow model. The comparison of global heat flux results in the wavy wall case with those of the horizontal flat wall case illustrated that, in a porous enclosure, the wavy wall reduced the heat transfer into the system. Kumar [12] studied free convection in a thermally stratified non-Darcian wavy porous enclosure. The effect of inertial forces due to non-Darcian Forchheimer term, thermal stratification level, vertical wavy wall amplitude, wave phase, roughness parameter, and Rayleigh number on the convection process was analyzed. The maximum influence of non-Darcian forces was noticed when wave phase of the wavy wall was around 300°. Recently, Sultana and Hyder [13] analyzed numerically non-Darcy natural convection inside a porous wavy-walled enclosure for various Darcy number and aspect ratio using one undulation. The enclosure consisted of two isothermal vertical wavy walls and two insulated horizontal walls. Their results showed that the wavy surface amplitude had a little influence on heat transfer distribution compared to the influence of Rayleigh and Darcy numbers. Chen et al. [14] analyzed numerically steady-state free convection inside a cavity made of two horizontal straight walls and two vertical bent-wavy walls and filled with a fluid-saturated porous medium. Their results showed that the dependence of the local Nusselt number on Darcy number and porosity was not small at large Darcy–Rayleigh number.

To the best of the authors' knowledge, no attention has been paid to non-Darcian effects on natural convection of flow and heat transfer in a cavity that is heated uniformly from a vertical wavy surface with different number of undulations and the wavy surface amplitude. The objective of the present study is to examine the momentum and energy transport processes inside a cavity made of two horizontal straight walls and filled with a fluid-saturated porous medium using different flow models of porous media such as Forchheimer-extended Darcy, Brinkman-extended Darcy, and the generalized model. The horizontal walls are kept adiabatic, while the vertical walls are isothermal but kept at different temperatures. The results are shown in terms of parametric presentations of streamlines and isotherms for various considered pertinent dimensionless parameters. These dimensionless groups include the Rayleigh number, the wavy surface amplitude, and number of undulations offered by the wavy vertical surface. Finally, the implications of the above dimensionless parameters are also depicted on the dimensionless local heat flux predictions.

2. Mathematical formulation

The problem under investigation is a laminar, steady, two dimensional natural heat transfer convection in a cavity filled with a porous medium. The physical system considered in the present investigation is illustrated in Fig. 1. The left wavy wall is maintained at a constant temperature T_H and the right wall is maintained at a constant temperature T_C, while maintaining $T_H > T_C$. The horizontal walls are considered adiabatic and impermeable.

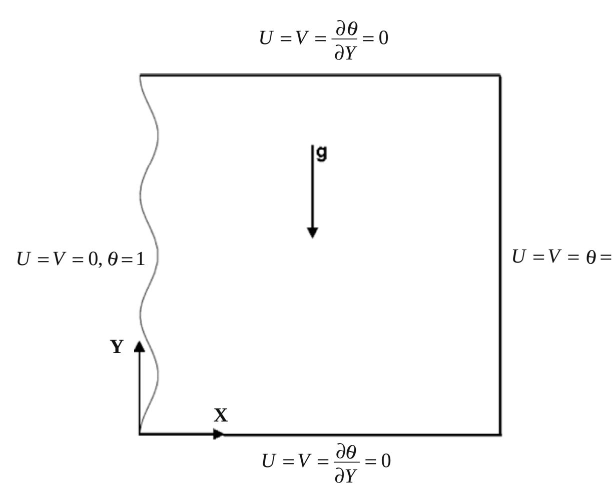

Fig. 1. Schematic diagram of the cavity and boundary conditions.

The thermophysical properties of the fluid are assumed constant, except for the density in the buoyancy term in the momentum equations which is treated according to Boussinesq model. Furthermore, the porous medium is considered homogeneous, isotropic and is saturated with a fluid that is in local thermodynamic equilibrium with the solid matrix of the porous medium.

By incorporating the above assumptions, the system of the governing equations can be expressed in canonical forms based on the volume average technique in the porous medium as such [15–19]:

Continuity equation:

$$\nabla \cdot < \mathbf{V} >= 0 \tag{1}$$

Momentum equation:

$$\frac{1}{\varepsilon}[< (\mathbf{V} \cdot \nabla)\mathbf{V} >] = -\nabla < \mathbf{P} >^f + \frac{1}{\varepsilon\sqrt{Ra/Pr}}\nabla^2 < \mathbf{V} > - \frac{< \mathbf{V} >}{Da\sqrt{Ra/Pr}} - \frac{F\varepsilon}{\sqrt{Da}}[< \mathbf{V} > \cdot < V >]J + \theta \tag{2}$$

Energy equation:

$$\mathbf{V} \cdot \nabla\theta = \frac{1}{\sqrt{PrRa}}\nabla^2\theta \tag{3}$$

The above equations were normalized using the following dimensionless parameters:

$$\mathbf{V} = \frac{\mathbf{v}}{\sqrt{g\beta\Delta TH}}, \quad P = \frac{p}{\rho(g\beta\Delta TH)}, \quad \theta = \frac{T - T_C}{T_H - T_C}, \quad \mathbf{x} = \frac{(x, y)}{H} \tag{4}$$

where β is the fluid thermal expansion coefficient, ρ the fluid density, g the gravitational acceleration, H is the height of the cavity, P the dimensionless pressure, $\mathbf{V}$ the dimensionless velocity vector, and $Da = K/H^2$ the Darcy number. In addition, the relevant Rayleigh number and Prandtl number are given by $Ra = g\beta\Delta TH^3/\nu\alpha$ and $Pr = \nu/\alpha$, respectively. The shape of the bottom wavy surface profile is assumed to mimic the following pattern

$$Y = A[1 - \cos(2n\pi X)] \tag{5}$$

where A is the dimensionless amplitude of the wavy surface and n is the number of undulation. The definition of the problem at hand is completed by highlighting the applied boundary conditions, which can be summarized as follows

$$\begin{aligned} &U = V = 0, \quad \theta = 1 \quad \text{at } X = 0,\ 0 < Y < 1 \\ &U = 0, V = 0, \quad \theta = 0 \quad \text{at } X = 1,\ 0 < X < 1 \\ &U = V = 0, \quad \frac{\partial\theta}{\partial Y} = 0 \quad \text{at } Y = 0,\ 0 \le X \le 1 \\ &U = V = 0, \quad \frac{\partial\theta}{\partial Y} = 0 \quad \text{at } Y = 1,\ 0 \le X \le 1 \end{aligned} \tag{6}$$

The rate of heat transfer is computed at the left vertical wall and is expressed in terms of the local Nusselt number Nu as

$$Nu = \frac{hH}{k} = -\frac{\partial\theta}{\partial n}H \tag{7}$$

where, h represents the heat transfer coefficient, k thermal conductivity and n the coordinate direction normal to the surface. The dimensionless normal temperature gradient can be written as

$$\frac{\partial\theta}{\partial n} = \frac{1}{H}\sqrt{\left(\frac{\partial\theta}{\partial X}\right)^2 + \left(\frac{\partial\theta}{\partial Y}\right)^2} \tag{8}$$

while the average Nusselt number ($\overline{Nu}$) is obtained by integrating the local Nusselt number along the left wavy surface and is defined by

$$\overline{Nu} = \frac{1}{S}\int_0^S Nu ds \tag{9}$$

where S is the total chord length of the wavy surface and s is the coordinate along the wavy surface.

3. Numerical scheme

A finite element formulation based on the Galerkin method is employed to solve the governing equations. The application of this technique is well documented by Taylor and Hood [20] and Gresho et al. [21]. In the current investigation, the continuum domain is divided into a set of non-overlapping regions called elements. Nine node quadrilateral elements with bi-quadratic interpolation functions are utilized to discretize the physical domain. Moreover, interpolation functions in terms of local normalized element coordinates are implemented to approximate the dependent variables within each element. Subsequently, substitution of the approximations into the system of the governing equations and boundary conditions yields a residual for each of the conservation equations. These residuals are then reduced to zero in a weighted sense over each element volume using Galerkin method.

The highly coupled and non-linear algebraic equations resulting from the discretization of the governing equations are solved using an iterative solution scheme called the segregated-solution algorithm. The advantage of using this method lies in that the global system matrix is decomposed into smaller submatrices and then solved in a sequential manner. This technique results in considerably fewer storage requirements. A pressure projection algorithm is utilized to obtain a solution for the velocity field at every iteration step. Furthermore, the pressure projection version of the

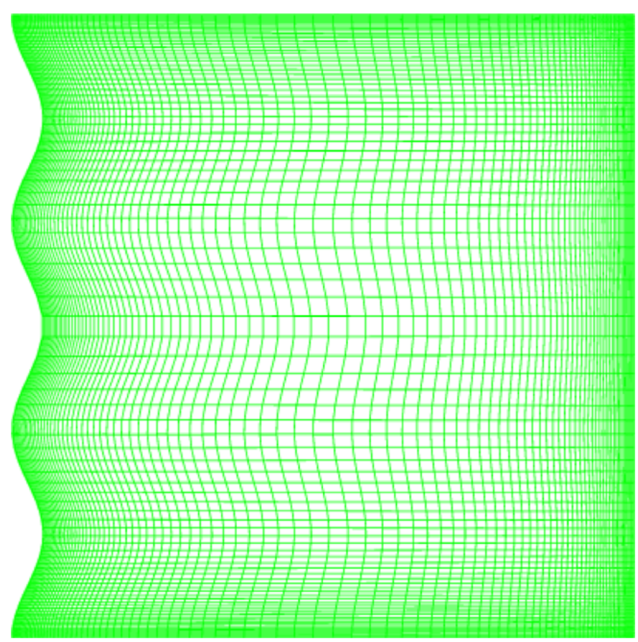

Fig. 2. Grid system used in the present study.

Table 1
Comparison of the average Nusselt number in a cavity filled with a porous medium between the present results and that of Nithiarasu et al. [21] and Chen et al. [13] for various Rayleigh numbers (ε = 0.9, $Da = 10^{-2}$).

Ra	$\overline{Nu}$ (Present)	$\overline{Nu}$ [22]	$\overline{Nu}$ [14]
1×10^3	1.02	1.023	1.02
1×10^4	1.63	1.63	1.63
1×10^5	3.93	3.91	3.92
5×10^5	6.69	6.70	NA

segregated algorithm is used to solve the non-linear system. In addition, the conjugate residual scheme is used to solve the symmetric pressure-type equation systems, while the conjugate gradient squared method is used for the non-symmetric advection-diffusion-type equations.

Many numerical experiments of various mesh sizes is performed to attain grid-independent results and to determine the best compromise between accuracy and minimizing computer execution time. As such, a variable grid-size system is employed in the present investigation to capture the rapid changes in the dependent variables especially near the walls where the major gradients occur inside the boundary layer (Fig. 2). To test and assess grid-independence of the solution scheme, numerical experiments were performed using various mesh size and found that 80 × 80 grid nodes (i.e., non-uniform spacing) was sufficient to produce grid-independence results.

Table 2
Comparison of the average Nusselt number in a cavity filled with a porous medium between the present results and that of Karimi–Farad [23] for various Darcy numbers ($Pr = Sc = 1$ & $Gr_T = Gr_C = 10^5$).

Da	$\overline{Nu}$ Present	$\overline{Nu}$ [23]	Difference (%)
10^{-2}	5.43	5.45	0.36
10^{-3}	3.54	3.63	2.54
10^{-4}	1.24	1.26	1.6

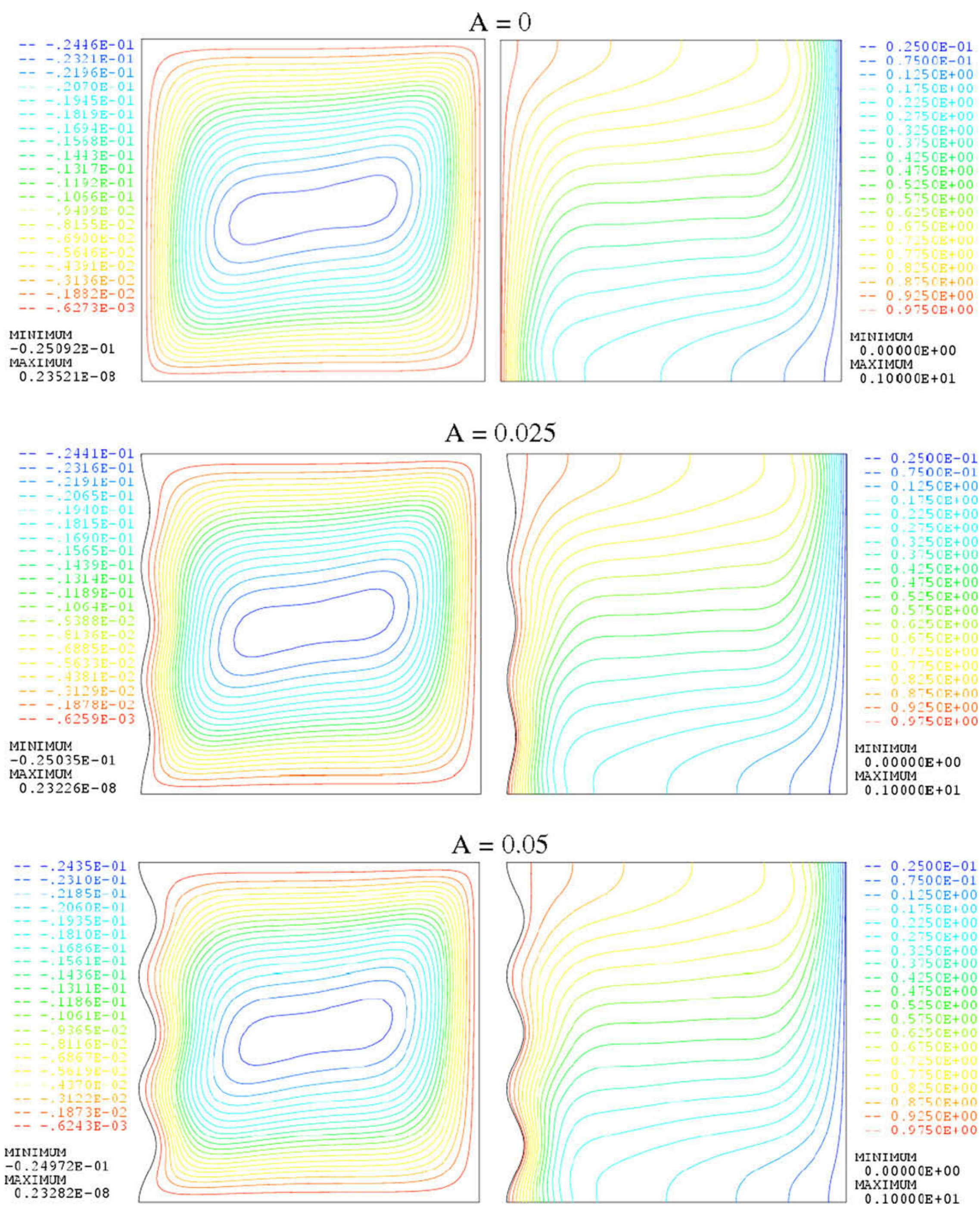

Fig. 3. Effect of varying the amplitude on the flow patterns and isotherms ($Da = 10^{-2}$, $Ra = 10^5$, $\varepsilon = 0.9$, $n = 3$).

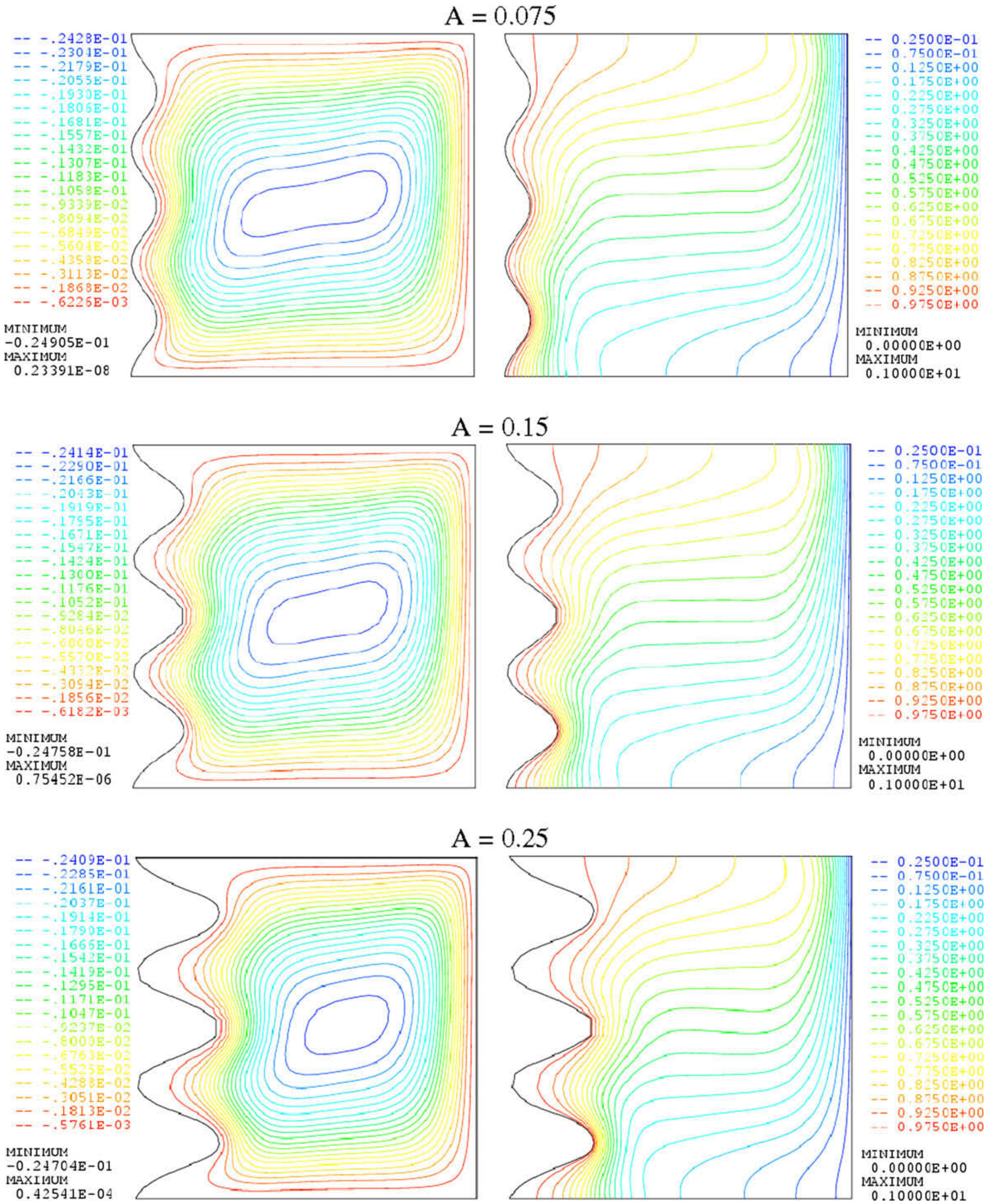

Fig. 3 (*continued*)

4. Validation

The present numerical code was validated against the numerical results of Nithiarasu et al. [22] and Chen et al. [14] for average Nusselt number using the generalized momentum equation of porous medium. Table 1, which demonstrates a comparison of the average Nusselt number between the present results and the numerical results of Nithiarasu et al. [22] and Chen et al. [14] reveals excellent agreement with the reported studies for various Rayleigh numbers. An additional check on the accuracy of the present code, the average Nusselt number results are also compared with the results reported by Karimi–Farad [23] on non-Darcian effects on double-diffusive convection within a porous medium. Table 2 demonstrates an excellent agreement between both results.

5. Results and discussion

The characteristics of the flow and temperature fields within the porous cavity were examined by exploring the effects of the Rayleigh number, number of undulations, and amplitude of the wavy surface. Such field variables were examined by outlaying the steady-state version of the streamline and temperature distributions as well as the local heat flux. In the current numerical

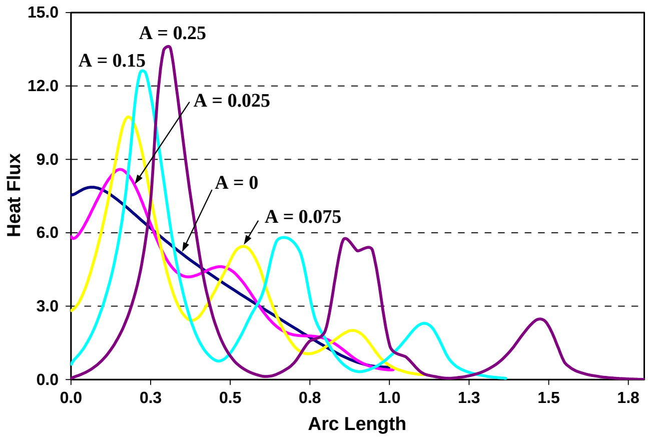

Fig. 4. The effect of A on the local heat flux ($Da = 10^{-2}$, $Ra = 10^5$, $\varepsilon = 0.9$, $n = 3$).

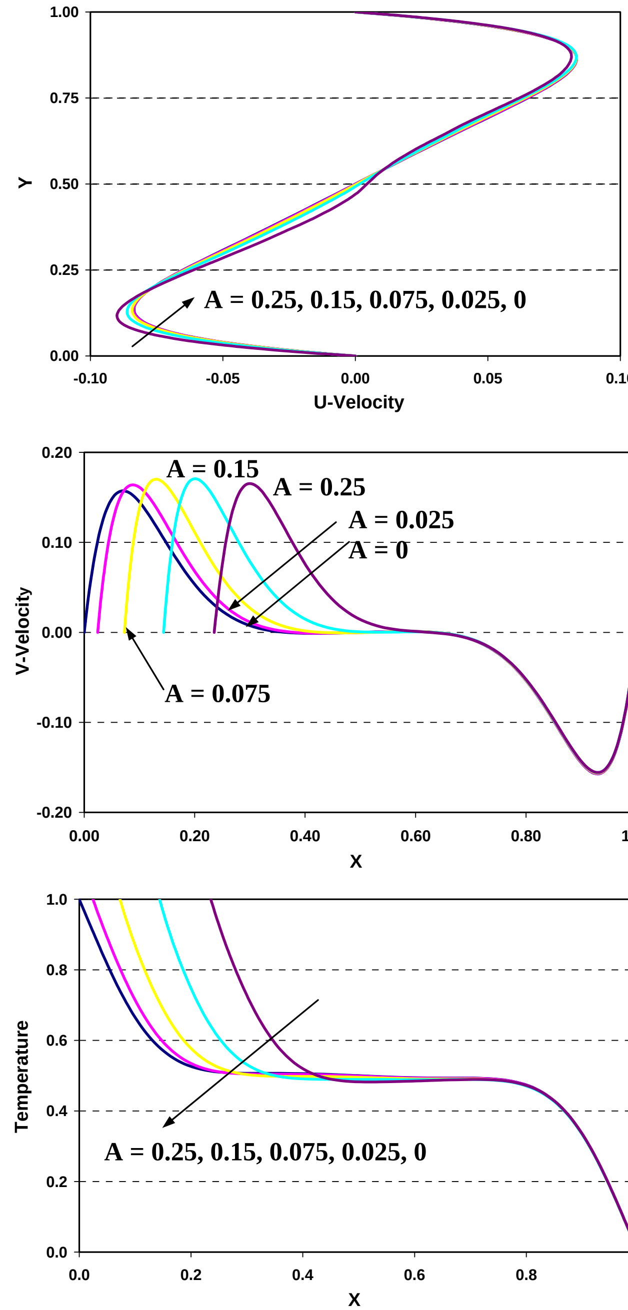

Fig. 5. The effect of A on the velocity and temperature profiles at mid-sections of the cavity ($Da = 10^{-2}$, $Ra = 10^5$, $\varepsilon = 0.9$, $n = 3$).

investigation, the following parametric domains of the dimensionless groups were considered: $10^4 \leq Ra \leq 10^6, 0 \leq n \leq 3, 0 \leq A \leq 0.25$. In addition, the maximum and minimum recirculation intensity levels and dimensionless temperature bounds were documented for the presented streamline results to reflect on the flow intensity levels. The effect of Darcy number and porosity on the heat transfer characteristics were not considered in the present work since their influence is well documented in the literature. As such $Da = 10^{-2}$ and $\varepsilon = 0.9$ were assumed in this study.

5.1. Effect of the wavy surface amplitude

The implications of the wavy surface amplitude A on the momentum and energy transport processes in the porous cavity is depicted in Fig. 3. This is first examined by plotting the streamlines and temperature contours as illustrated in Fig. 3. The results, which are depicted for $Ra = 10^5$ and $n = 3$, indicate that the flow activities and thermal currents are both a weak function of surface amplitude in the considered rage of $A = 0$–0.25 This effect is more profound in Fig. 4 which shows the effect of the wavy surface amplitude on the local variation of heat flux along the wavy surface. The results in Fig. 4 exhibit higher local heat flux variation with an increase in the amplitude of the wavy surface owing to higher velocity gradients near the wavy surface which subsequently increases the heat transfer rate. Moreover, Fig. 4 demonstrates that the heat flux is higher close to the lower edge of the vertical wavy wall for various amplitudes. The effect of the wavy surface amplitude on the velocity and temperature profiles at mid-sections of the cavity is illustrated in Fig. 5. This figure shows that the amplitude of the wavy surface has an effect on the flow velocity and temperature next to the wavy surface.

5.2. Effect of the Rayleigh number and the number of undulations on the streamlines and isotherms

The effect of Rayleigh number on the streamline contours and isotherms is depicted in Figs. 6 and 7. These figures show that for low values of Rayleigh number, a central vortex appears as the dominant characteristic of the flow. As Rayleigh number increases ($Ra = 10^4$), the vortex tends to become elliptic and finally breaks up into two vortices and move towards the vertical walls at high Rayleigh number ($Ra = 10^6$). The shape of the isotherms shows how the dominant heat transfer mechanism changes as Rayleigh number increases. For low Ra-values almost vertical isotherms appear, because heat is transferred by conduction between hot and cold walls. As the isotherms depart from the vertical position ($Ra = 10^4$), the heat transfer mechanism changes from conduction to convection. Fig. 7 shows that the isotherms at the centre of the cavity are horizontal and become vertical only inside the very thin boundary layers at $Ra = 10^6$. The effect of the number of undulations on the streamlines and isotherms is shown in Figs. 6 and 7 for various Rayleigh number. It appears from the figures that varying the number of undulations between 0 and 3 does not disturb the global flow and isotherm patterns except in the vicinity of the vertical wavy wall, where the contour lines mimic the wall's profile. In addition, the recorded upper and lower bounds for flow intensities do not seem to vary significantly for Rayleigh number of 10^4. However, at Rayleigh number of 10^6, Fig. 7 illustrates that the presence of undulations influence the shape and the size of the vortex next to the wavy surface.

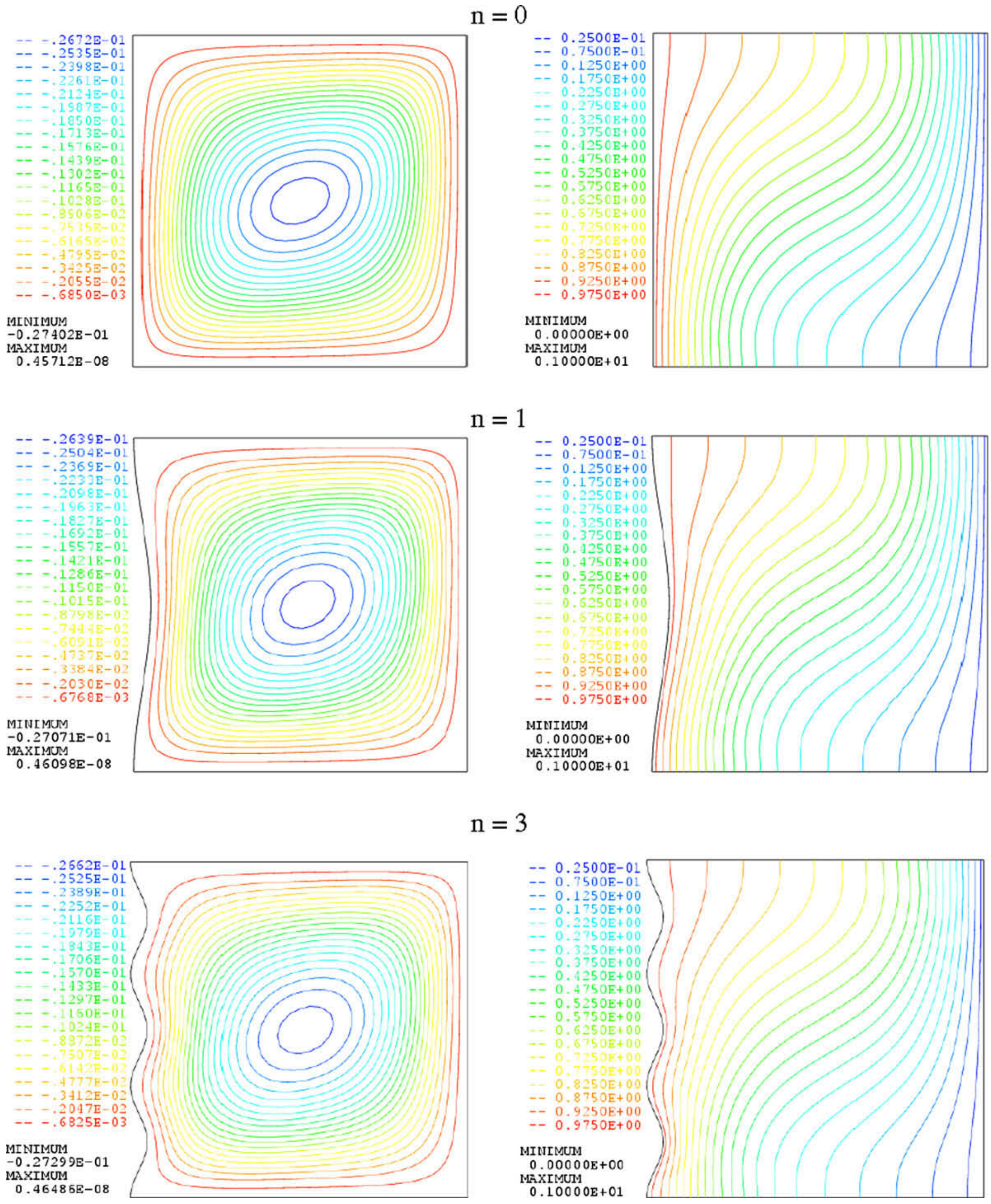

Fig. 6. Effect of varying *n* on the flow patterns and isotherms ($Da = 10^{-2}$, $Ra = 10^4$, $\varepsilon = 0.9$, $A = 0.05$).

5.3. Effect of the Rayleigh number and the number of undulations on the local heat flux

The influence of the number of undulation on the local heat flux for various Rayleigh numbers is demonstrated in Figs. 8 and 9. These figures show that the employed number of undulation impacts the distribution of the local heat flux along arc length of the vertical surface by producing a corresponding number of peaks and valleys which correspond to the imposed *n* values. Moreover, the local heat flux increases along the segments of the wavy wall entering into the fluid domain and decreases along the segments of the wavy wall protruding out of the domain. It is worth mentioning that the local heat flux is higher close to the bottom of the vertical wall and this is associated with a fact that the clockwise rotating fluid carries energy from the left wavy wall and, consequently, becomes hot as it rises up again. Therefore, the local heat flux along the wavy wall decreases as the temperature difference between the fluid and the wall decreases. Figs. 8 and 9 illustrate that the steep rise in the local heat flux along the wavy wall for $n = 3$ is seen to decrease as n decreases.

5.4. Effect of the Rayleigh number and the number of undulations on the average Nusselt number

The effect of varying Rayleigh number and the number of undulations on the average Nusselt number of the wavy left wall

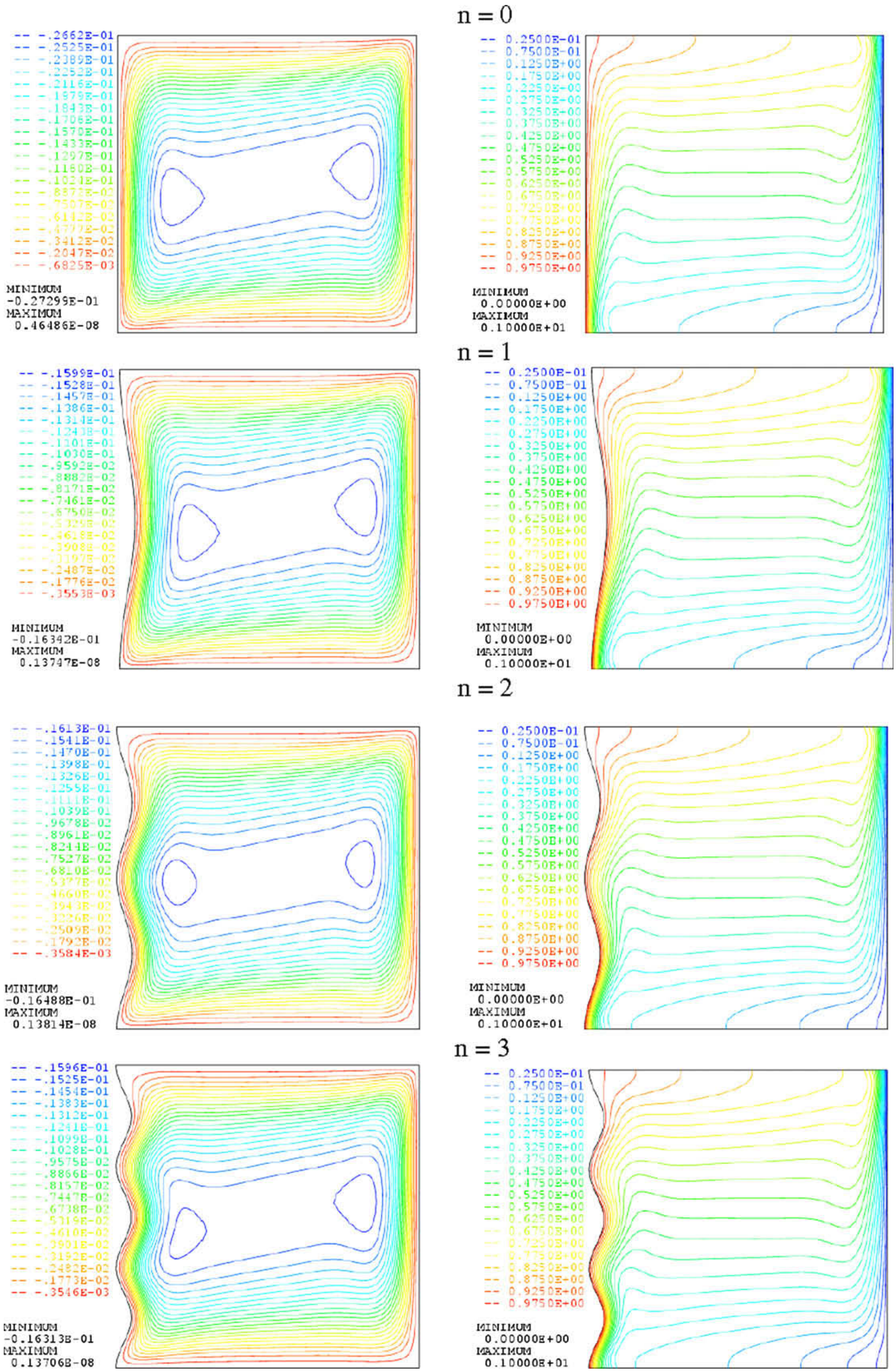

Fig. 7. Effect of varying n on the flow patterns and isotherms ($Da = 10^{-2}$, $Ra = 10^{6}$, $\varepsilon = 0.9$, $A = 0.05$).

normalized by the corresponding average Nusselt number for a smooth wall is illustrated in Fig. 10. This figure shows that the wavy wall has a slight effect on the average Nusselt number compared with a smooth wall case.

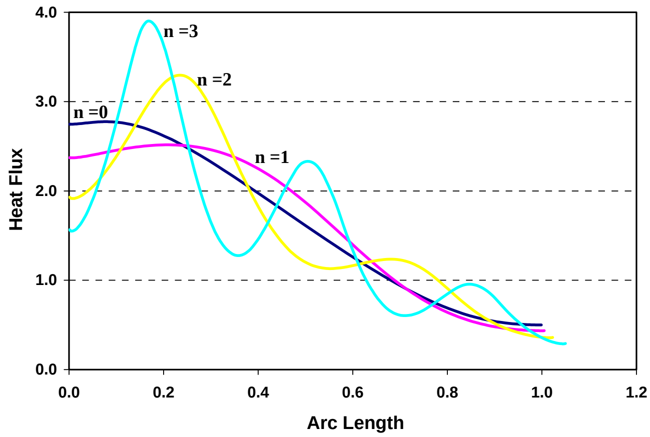

Fig. 8. Effect of varying n on the heat flux ($Da = 10^{-2}$, $Ra = 10^4$, $\varepsilon = 0.9$, $A = 0.05$).

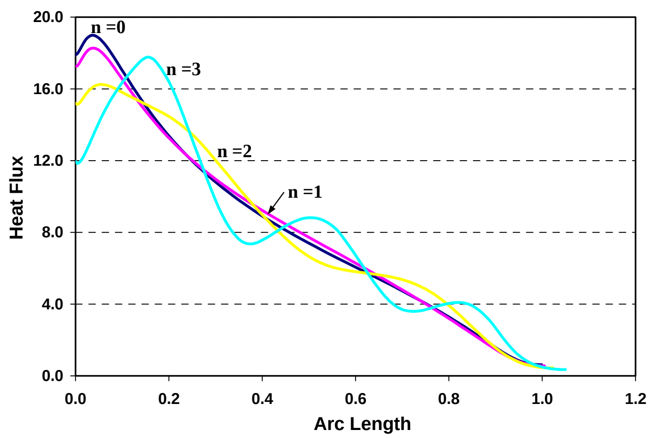

Fig. 9. Effect of varying n on the heat flux ($Da = 10^{-2}$, $Ra = 10^6$, $\varepsilon = 0.9$, $A = 0.05$).

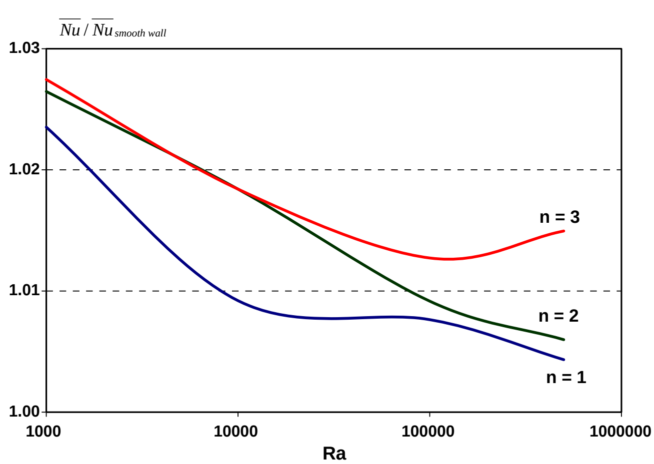

Fig. 10. Effect of Rayleigh number and the number of undulations on the average Nusselt number normalized by the corresponding average Nusselt number for a smooth wall ($Da = 10^{-2}$, $\varepsilon = 0.9$, $A = 0.05$).

5.5. Effect of varying the flow model for porous media on the average Nusselt number

Fig. 11 illustrates the effect of varying Rayleigh number on the average Nusselt number using different flow models for porous media such as Forchheimer's extension, Brinkman's extension, and the generalized model. Non-Darcian effects are analyzed through investigating the average Nusselt number. It is interesting to note that Brinkman's extension of the Darcy model and the generalized model are very close. For wavy left wall, the use of the Forchheimer's extension results in an overestimation for the average Nusselt number compared to models based on Brinkman's extension and the generalized model.

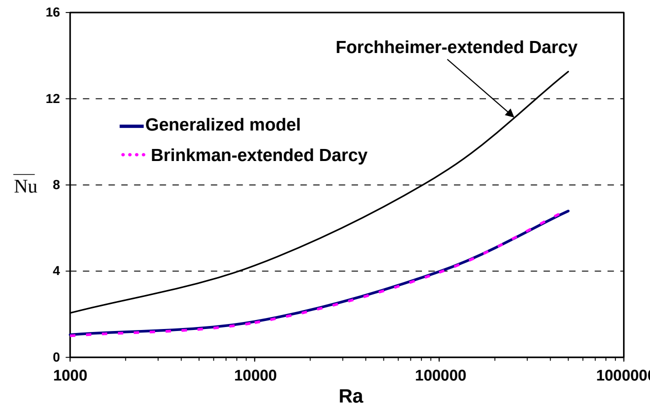

Fig. 11. Effect of varying Rayleigh number on the average Nusselt number using different flow models for porous media ($Da = 10^{-2}$, $\varepsilon = 0.9$, $A = 0.05$, $n = 3$). Wavy left wall.

Table 3
Effect of varying the location of the wavy surface on the average Nusselt number ($Da = 10^{-2}$, $\varepsilon = 0.9$, $A = 0.05$).

Ra	$\overline{Nu}$ (smooth left wall)	$\overline{Nu}$ (wavy left wall)	$\overline{Nu}$ (wavy bottom wall)
1×10^3	1.02	1.048	0.98
1×10^4	1.63	1.66	1.567
1×10^5	3.93	3.98	3.83
5×10^5	6.69	6.79	6.55

5.6. Effect of the wavy surface location on the average Nusselt number

Table 3 demonstrates the effect of varying the wavy surface location on the average Nusselt number compared with the results for a smooth wall. The results show that the boundary condition at the left wavy wall has an insignificant effect on the average Nusselt numbers compared with a smooth left wall case for the range of Rayleigh numbers studied in this work. However, this table shows that bottom wavy surface has a slight effect on the average Nusselt number when the left wall kept at a high temperature; T_H.

6. Conclusions

Natural convection heat transfer in a wavy cavity filled with a porous-saturated medium was studied numerically for various pertinent dimensionless groups. The vertical surface was considered to follow a wavy pattern. Furthermore, the horizontal walls were subjected to insulated boundary conditions. The generalized model of the momentum equation, which is also known as the Forchheimer–Brinkman-extended Darcy model was solved using the Galerkin finite element method. Effects of dimensionless groups representing the wavy geometry, Rayleigh number, and number of undulation were highlighted to study their impacts on flow structure and heat transfer characteristics. The results of this investigation illustrated that the amplitude of the wavy surface and the number of undulations affect heat transfer characteristics inside the cavity. Furthermore, the intensity of convection within the cavity was observed to increase with the increase in the Rayleigh number. A comparison of the several flow models for porous media such as Forchheimer-extended Darcy, Brinkman-extended Darcy, and the generalized flow models was conducted to show the influence of non-Darcian effects on the average Nusselt number.

References

[1] J.-H. Jang, W.-M. Yan, Mixed convection heat and mass transfer along a vertical wavy surface, Int. J. Heat Mass Transfer 47 (2004) 419–428.
[2] P.K. Das, S. Mahmud, Numerical investigation of natural convection inside a wavy enclosure, Int. J. Therm. Sci. 42 (2003) 397–406.
[3] L. Adjlout, O. Imine, A. Azzi, M. Belkadi, Laminar natural convection in an inclined cavity with a wavy-wall, Int. J. Heat Mass Transfer 45 (2002) 2141–2152.
[4] S. Mahmud, P.K. Das, N. Hyder, A.K. M Islam, Free convection in an enclosure with vertical wavy walls, Int. J. Therm. Sci. 41 (2002) 440–446.
[5] A. Dalal, M.K. Das, Natural convection in a cavity with a wavy wall heated from below and uniformly cooled from the top and both sides, J. Heat Transfer 128 (2006) 717–725.
[6] A. Misirlioglu, A.C. Baytas, I. Pop, Natural convection inside an inclined wavy enclosure filled with a porous medium, Transport Porous Media 64 (2006) 229–246.
[7] A. Misirlioglu, A.C. Baytas, I. Pop, Free convection in a wavy cavity filled with a porous, Int. J. Heat Mass Transfer medium 48 (2005) 1840–1850.
[8] B.V. Ratish Kumar, P.V.S.N. Murthy, P. Singh, Free convection heat transfer from an isothermal wavy surface in a porous enclosure, Int. J. Numer. Meth. Fluids 28 (1998) 633–661.
[9] B.V. Rathish Kumar, Shalini, Free convection in a non-Darcian wavy porous enclosure, Int. J. Eng. Sci. 41 (2003) 1827–1848.
[10] B.V. Rathish Kumar, A study of free convection induced by a vertical wavy surface with heat flux in a porous enclosure, Numer. Heat Transfer A: Appl. 37 (2000) 493–510.
[11] P.V.S.N. Murthy, B.V. Rathish Kumar, P. Singh, Natural convection heat transfer from a horizontal wavy surface in a porous enclosure, Numer. Heat Transfer A: Appl. 31 (1997) 207–221.
[12] B.V. Rathish Kumar, Free convection in a thermally stratified non-Darcian wavy porous enclosure, J. Porous Media 7 (2004) 1–12.
[13] Z. Sultana, N. Hyder, Non-Darcy free convection inside a wavy enclosure, Int. Commun. Heat Mass Transfer 34 (2007) 136–146.
[14] X.B. Chen, P. Yu, S.H. Winoto, H.T. Low, Free convection in a porous cavity based on the Darcy-Brinkman–Forchheimer extended model, Numer. Heat Transfer A 52 (2007) 377–397.
[15] K. Khanafer, K. Vafai, The role of porous media in biomedical engineering as related to magnetic resonance imaging and drug delivery, Heat Mass Transfer 42 (2006) 939–953.
[16] A. Amiri, K. Vafai, Analysis of dispersion effects nonthermal equilibrium non-Darcian variable porosity incompressible-flow through porous-media, Int. J. Heat Mass Transfer 37 (1994) 939–954.
[17] A. Amiri, K. Vafai, Transient analysis of incompressible flow through a packed bed, Int. J. Heat Mass Transfer 41 (1998) 4259–4279.
[18] K. Vafai, C.L. Tien, Boundary and inertia effects on convective mass transfer in porous media, Int. J. Heat Mass Transfer 25 (1981) 1183–1190.
[19] K. Vafai, C.L. Tien, Boundary and inertia effects on flow and heat transfer in porous media, Int. J. Heat Mass Transfer 24 (1980) 195–203.
[20] C. Taylor, P. Hood, A numerical solution of the Navier–Stokes equations using finite-element technique, Comput. Fluids 1 (1973) 73–89.
[21] P.M. Gresho, R.L. Lee, R.L. Sani, On the time-dependent solution of the incompressible Navier–Stokes equations in two and three dimensions, in: Recent Advances in Numerical Methods and Fluids, Pineridge, Swansea, UK, 1980.
[22] P. Nithiarasu, K.N. Seetharanu, T. Sundararajan, Natural convective heat transfer in a fluid saturated variable porosity medium, Int. J. Heat Mass Transfer 40 (1997) 3955–3967.
[23] M. Karimi-Fard, M.C. Charrier-Mojtabi, K. Vafai, Non-Darcian effects on double-diffusive convection within a porous medium, Numerical Heat Transfer Journal 31 (1997) 837–852.